



## Effect of titanium dioxide nanotubes on the mechanical and antibacterial properties of the low-viscosity bulk-fill composite

Rumeysa Hatice Enginler Ozlen, Evrim Eliguzeloglu Dalkilic, Bedri Onur Kucukyildirim, Ayşegül Akdoğan Eker, Nursen Topcuoğlu & Guven Kulekci

**To cite this article:** Rumeysa Hatice Enginler Ozlen, Evrim Eliguzeloglu Dalkilic, Bedri Onur Kucukyildirim, Ayşegül Akdoğan Eker, Nursen Topcuoğlu & Guven Kulekci (2022) Effect of titanium dioxide nanotubes on the mechanical and antibacterial properties of the low-viscosity bulk-fill composite, *Journal of Adhesion Science and Technology*, 36:16, 1727-1744, DOI: [10.1080/01694243.2021.1982282](https://doi.org/10.1080/01694243.2021.1982282)

**To link to this article:** <https://doi.org/10.1080/01694243.2021.1982282>



Published online: 23 Oct 2021.



Submit your article to this journal [↗](#)



Article views: 282



View related articles [↗](#)



View Crossmark data [↗](#)








Citing articles: 1 View citing articles [↗](#)



ARTICLE



## Effect of titanium dioxide nanotubes on the mechanical and antibacterial properties of the low-viscosity bulk-fill composite

Rumeysa Hatice Enginler Ozlen<sup>a</sup>, Evrim Eliguzeloglu Dalkilic<sup>b</sup> ,  
Bedri Onur Kucukyildirim<sup>c</sup> , Ayşegül Akdoğan Eker<sup>c</sup> , Nursen Topcuoğlu<sup>d</sup>   
and Guven Kulekci<sup>d</sup> 

<sup>a</sup>Department of Restorative Dentistry, Restorative Dentistry Specialist, Bezmialem Vakif University Faculty of Dentistry, Istanbul, Turkey; <sup>b</sup>Department of Restorative Dentistry, Bezmialem Vakif University Faculty of Dentistry, Istanbul, Turkey; <sup>c</sup>Department of Mechanical Engineering, Yildiz Technical University, Istanbul, Turkey; <sup>d</sup>Department of Oral Microbiology, Istanbul University Faculty of Dentistry, Istanbul, Turkey;

### ABSTRACT

The purpose of this investigation is to determine the impact of titanium dioxide nanotubes (TiO<sub>2</sub>-n) on the mechanical and antibacterial properties of bulk-fill composite resin. TiO<sub>2</sub>-n were synthesized in laboratory conditions using the hydrothermal method. Varying amounts of TiO<sub>2</sub>-n were included in the bulk-fill composite resin. Microhardness, surface roughness, and the three-point bending test were used to determine the mechanical properties of the composite. After the flexural strength test, the fractured surfaces of the composite resin were examined with a high-resolution scanning electron microscope. The antibacterial activity of *Streptococcus mutans* (*S.mutans*) and *Lactobacillus Casei* (*L.casei*) was assessed using a direct contact test. The statistical examination was completed using IBM SPSS Statistics 22. Group differences were compared using the Kruskal Wallis and Dunn tests ( $p < 0.05$ ). The addition of TiO<sub>2</sub>-n did not change the roughness of the bulk-fill composites ( $p > 0.05$ ). Adding 0.5% and 1% TiO<sub>2</sub>-n increased the microhardness of the bulk-fill composite ( $p < 0.05$ ). Adding TiO<sub>2</sub>-n did not change the three-point bending results of the bulk-fill composite ( $p > 0.05$ ). Though adding TiO<sub>2</sub>-n did not have an antibacterial impact on *S.mutans* ( $p > 0.05$ ), adding 0.5% TiO<sub>2</sub>-n produced an antibacterial impact on *L.casei* in daylight ( $p < 0.05$ ). The addition of 0.5% and 1% TiO<sub>2</sub>-n increased the microhardness of the top surface of the bulk-fill composite without negatively affecting surface roughness or the composite's three-point bending properties. Adding 0.5% TiO<sub>2</sub>-n to the composite resin produced an antibacterial impact on *L.casei* in daylight.

### ARTICLE HISTORY

Received 10 July 2021  
Revised 10 September 2021  
Accepted 14 September 2021

### KEYWORDS

TiO<sub>2</sub>-n; nanotube; bulk-fill composite resin; three-point bending; microhardness; surface roughness

## 1. Introduction

Composite resins are preferred in aesthetic dentistry because they offer mechanical and physical properties similar to dental tissues, possess good aesthetic properties, and offer sufficient resistance to chewing forces [1]. Traditional composite resin materials should be placed in the cavity in 2-mm layers. However, applying a dental composite using this type of incremental placement technique requires light-curing each increment individually and is time-consuming for the patient and the dentist. There is also an increased possibility of air bubble inclusion or moisture contamination between individual increments of resin composite restoration [2]. The development of composite resins has come to the fore for counteracting the adverse effects of layering technique and polymerization shrinkage [3–6]. Bulk-fill composites are divided into two categories with mechanical and physical properties that vary according to the inorganic filler content [7]. These categories consist of high-viscosity (condensed) bulk-fill composites and low-viscosity bulk-fill composites. Low-viscosity bulk-fill composites have advantages like low elastic modulus; lower stress during polymerization shrinkage; and better adaptation to cavity walls, especially on irregular surfaces [8,9].

Despite the many advantages and widespread clinical application of composite resins in recent years, there are still some limitations to their clinical performance. These limitations can cause restorations made with composite resins to fail and may result in restorations that must be changed. The two main causes of failure reported in the literature are secondary caries and fractures [10–14]. In addition, composite resins tend to form more biofilms than other restorative materials and tooth enamel [15,16]. High biofilm accumulation in composite resin restoration may contribute to the progression of secondary caries [17].

To improve the mechanical and antibacterial properties of composites, various materials have been added to composite resins, including metal oxides such as nanofiller, glass fiber, silver, and titanium dioxide nanotubes ( $\text{TiO}_2\text{-n}$ ) [18–21]. Unlike nanoparticles, nanotubes are characterized by a high surface-to-volume ratio. The hollow structure of the nanotubes provides space to interlock with the matrix on the inner and outer surfaces of the pipes [22]. As a result, higher interface amounts improve the mechanical properties of composite resin material [23].

Previous studies have explored improving the general performance of dental materials by adding  $\text{TiO}_2\text{-n}$  to polymeric materials [24–28]. One recent study reported that when  $\text{TiO}_2\text{-n}$  was added to a low-viscosity dental composite, three-point bending and fracture strength were improved [26]. Yu et al. reported that the use of 0.1%, 0.25%, and 0.5%  $\text{TiO}_2\text{-n}$  resulted in a significant change in the mechanical properties of experimental composite resins. The addition of functionalized or non-functionalized  $\text{TiO}_2$  nanoparticles to composite resins has been shown to increase both the mechanical performance and the antibacterial potential of composites [29–32]. It has also been reported that the addition of functionalized  $\text{TiO}_2$  nanoparticles to dental adhesives can prolong the clinical life of restorations [25,33]. Generally, methacrylate acid is used for the functionalization of  $\text{TiO}_2\text{-n}$ . However, this functionalization requires an additional step. There are a limited number of studies on the addition of  $\text{TiO}_2\text{-n}$  to bulk-fill composites. The purpose of this study is to evaluate the microhardness, surface roughness,

three-point bending, and antibacterial properties of low-viscosity bulk-fill composite resin with and without different proportions of TiO<sub>2</sub>-n in functional groups.

The null hypotheses of this study are as follows:

1. The addition of TiO<sub>2</sub>-n in different proportions increases the microhardness of low-viscosity bulk-fill composite resin.
2. The addition of TiO<sub>2</sub>-n in different proportions does not affect the surface roughness of low-viscosity bulk-fill composite resin.
3. The addition of TiO<sub>2</sub>-n in different proportions does not affect the three-point bending of low-viscosity bulk-fill composite resin.
4. The addition of TiO<sub>2</sub>-n in different proportions to the low-viscosity bulk-fill composite is effective against *S.mutans* and *L.casei*.

## 2. Materials and methods

### 2.1. Synthesis of TiO<sub>2</sub>-n

Titanium dioxide nanopowder (anatase; particle size < 25 nm; 99.7% purity) was used for the synthesis of titanium dioxide nanotubes (Sigma-Aldrich, Taufkirchen, Germany). A hydrothermal synthesis method was used to synthesize TiO<sub>2</sub>-n due to its ease of use. All operations prior to nanotube production were carried out in the fume hood with the necessary safety measures. A total of 120 mL of 10 M NaOH solution was prepared, and 1.2 grams of TiO<sub>2</sub> nanoparticles were added to the alkaline solution. The solution obtained was subjected to homogenization in an ultrasonic bath for 1 h to prevent nanoparticle clustering. At this point, the solution was ready for hydrothermal synthesis and was thus connected to the reflux device. Additional hydroxylic functional groups on the surface of synthesis products can be obtained using a reflux tube. Obtaining functional groups during synthesis in nanotubes reduced possible agglomeration without any additional functionalization process. The solution was first kept at 30 °C for 2 h and then was brought to 110 °C and held for 72 h using a heater with a magnetic stirrer. After this, the solution was diluted with distilled water using the filtration apparatus. Dilution continued until the pH was neutralized. The TiO<sub>2</sub>-n mixture was obtained as a result of filtration, transferred to the ceramic evaporator vessel, and kept in a 120 °C oven for 14–16 h to evaporate all water.

### 2.2. Characterization of TiO<sub>2</sub>-n

Characterization of TiO<sub>2</sub>-n was performed using Fourier-transform infrared (FTIR) spectroscopy (100 FTIR Spectrometry, Perkin Elmer, USA) and Raman Spectroscopy (Renishaw Streamline, Germany) devices. To determine the morphology of the TiO<sub>2</sub>-n, a high-resolution scanning electron microscope (SEM) was used (FEI brand QUANTA FEG 250 ESEM, FEI, USA) with high vacuum mode (110 Pa pressure), a high vacuum detector at 30 kV voltage, and 3.0 spot values, and 50,000x and 400,000× magnification.

### **2.3. Adding TiO<sub>2</sub>-n to composite resin**

The TiO<sub>2</sub>-n was transformed into an acetone solution and subjected to probe homogenization for 10 min to prevent clustering over time. The solution was then heated to remove the acetone. The TiO<sub>2</sub> percentage was calculated according to the weight of the composite to be used at 0.1%, 0.5%, and 1%, and the TiO<sub>2</sub>-n was weighed using a precision scale. The TiO<sub>2</sub>-n was then manually added to the low-viscosity bulk-fill composites (Estelite Bulk-Fill Flow, Tokuyama Corp, Japan) (A2 Shade) and handled with speculation for 20 min. Three experimental groups were prepared using these composites, and one control group was prepared using a composite without TiO<sub>2</sub>-n.

### **2.4. Surface roughness test**

The samples were prepared by one researcher (R.Ö.) Samples were prepared in cylindrical Teflon molds (2 mm height and 10 mm diameter) using a transparent matrix strip and rigid microscope slides on both surfaces ( $n = 6$ ). The samples were then polymerized with an LED light device for 20 sec. Polymerization was performed by positioning the light guide tip so that it was in contact with the glass slide on the top surface of the specimen. The upper surface of the specimens was polished with aluminum oxide polishing discs (Sof-lex, 3 M ESPE, USA) for 10 sec in accordance with the manufacturer's instructions, progressing from coarse to fine. After each disc application, the samples were washed with an air-water spray and dried. The discs were renewed after each use. All samples were stored in an opaque glass bottle in distilled water at 37 °C. Surface roughness was measured three times from different areas using the profilometer device Mahr M300C (Carl-Mahr, Germany). Mean and standard deviation values were determined in Ra.

### **2.5. Vickers microhardness test**

Composite samples were prepared using the same cylindrical Teflon molds (2 mm height and 10 mm diameter;  $n = 6$ ). Vickers hardness measurements were performed on the bottom and top surfaces of all samples at a load of 200 g for 15 sec (Shimadzu, Tokyo, Japan). Three measurements were taken from three different regions, and the average of these measurements was calculated.

### **2.6. Three-Point bending test**

For the three-point bending test, a specially designed stainless steel mold (2 × 2 × 25 mm) that met ISO standards (4049: 2009) was used [34]. A metal mold was placed on the transparent band on the rigid microscope slide, and flowable bulk-fill composite resin was placed into the mold. A smooth surface was created by placing transparent tape and a microscopic slide on top again. Samples from five different regions were polymerized for 20 sec each using an LED light device ( $n = 8$ ) [35]. The prepared samples were kept in distilled water at 37 °C for 24 h in an opaque glass bottle. Samples were subjected to three-point bending on a 15-mm device in a universal testing machine (Shimadzu, Japan), and flexural force was applied at a speed of 1 mm/min

[35]. The maximum force value at which the fracture occurred was recorded in Newton units. The following formula was used when calculating the flexural strength in MPa ( $\sigma$ ).

$$\sigma = 3FL/2wh^2$$

$\sigma$ : Flexural strength

F: Maximum force at break (N)

L: Width of the test setup where the force is applied (mm)

w: Width of the sample (mm)

h: Thickness of sample (mm)

The fracture surfaces were examined by HR-SEM (FEI brand QUANTA FEG 250 ESEM, FEI, USA).

### 2.7. Direct contact test

Two different bacterial species, *Streptococcus mutans* (ATCC 25175) and *Lactobacillus casei* (ATCC 4646), were selected to evaluate the antibacterial effectiveness of bulk-fill composite resin materials with TiO<sub>2</sub>-n added in different percentages. The antibacterial activities of the prepared composite resins were evaluated using a direct contact test.

The direct contact test was carried out according to the guidelines provided by Weiss et al. (1996). For each study and control group, the bottoms of 11 wells in a 96-well sterile ELISA plate were covered with the materials. The ELISA plates were sterilized using H<sub>2</sub>O<sub>2</sub> gas plasma sterilization. 10  $\mu$ l of bacterial suspension prepared with 24 hr cultures of each bacteria resuspended in fresh brain heart infusion (BHI; Merck Darmstadt, Germany) broth (approximately 10<sup>6</sup> cfu/ml) were placed directly on each material. In addition, a positive control group was formed by adding 10  $\mu$ l of bacteria suspension to 10 material-free wells. A negative control group was formed by adding sterile broth to the single remaining material-covered well. The bacterial suspension was kept at 37 °C for 1 h in a humid environment on a shaker to allow the liquid to evaporate. BHI broth (200  $\mu$ l) was added to each of the wells and gently stirred for 2 min; 10  $\mu$ l were then transferred to another plate with an adjacent set of wells containing fresh medium (200  $\mu$ l), and the materials were mixed. The growth kinetics of bacteria was monitored using a microplate spectrophotometer at 620 nm wavelength (Genesys™ 10S UV-Vis, Thermo Scientific, USA) every 3 hr for a total of 24 hr. Automixing prior to each reading ensured homogeneous bacterial cell suspension. Data were recorded according to the optical density values obtained.

### 2.8. Statistical analysis

To evaluate the findings, IBM SPSS Statistics 22 (SPSS IBM, Turkey) programs were used. The suitability of the parameters for the assumption of a normal distribution was evaluated with the Shapiro-Wilks test. The Kruskal-Wallis test was used to compare parameters between groups, and Dunn's test was used to determine the group that caused the difference. The Mann-Whitney U test was used for upper and lower surface

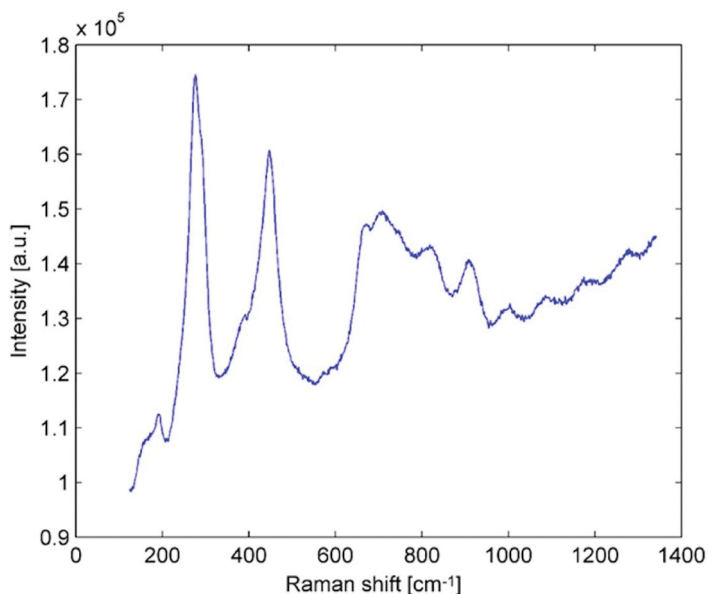


**Figure 1.** Raman spectroscopy of TiO<sub>2</sub>-n.

comparisons, while the Friedman test and Wilcoxon sign test were used for in-group comparisons of parameters. Significance was evaluated at the  $p < 0.05$  level.

### 3. Results

#### 3.1. Characterization of TiO<sub>2</sub>-n

The crystalline phase of the TiO<sub>2</sub>-n synthesized with the hydrothermal technique was determined by Raman spectroscopy and FTIR analyses. **Figure 1** presents the results of the Raman spectroscopy, with the peaks indicating that the TiO<sub>2</sub>-n has an anatase crystal structure.

The FTIR spectra show the formation of peaks at wavelengths of 3366 cm<sup>-1</sup>, 1635 cm<sup>-1</sup>, and 975 cm<sup>-1</sup>, demonstrating that TiO<sub>2</sub>-n with H-O-H and -OH bonds were obtained (**Figure 2**). The presence of C=C vinyl bands was detected with bands at a wavelength of 1635 cm<sup>-1</sup>. O-H bands were detected at the 3366 cm<sup>-1</sup> wavelengths, while C-C and C=C stretching vibrations produced the bands seen at the 975 cm<sup>-1</sup> wavelengths.

#### 3.2. Scanning electron microscopy (SEM)

The morphology of the TiO<sub>2</sub>-n powder obtained using the hydrothermal synthesis method was determined *via* SEM. SEM images were taken at 400,000 $\times$  magnification. The micrographs obtained *via* SEM are presented in **Figure 3** and confirm the hollow tubular structure of TiO<sub>2</sub>-n in the size range of 15–20 nm.

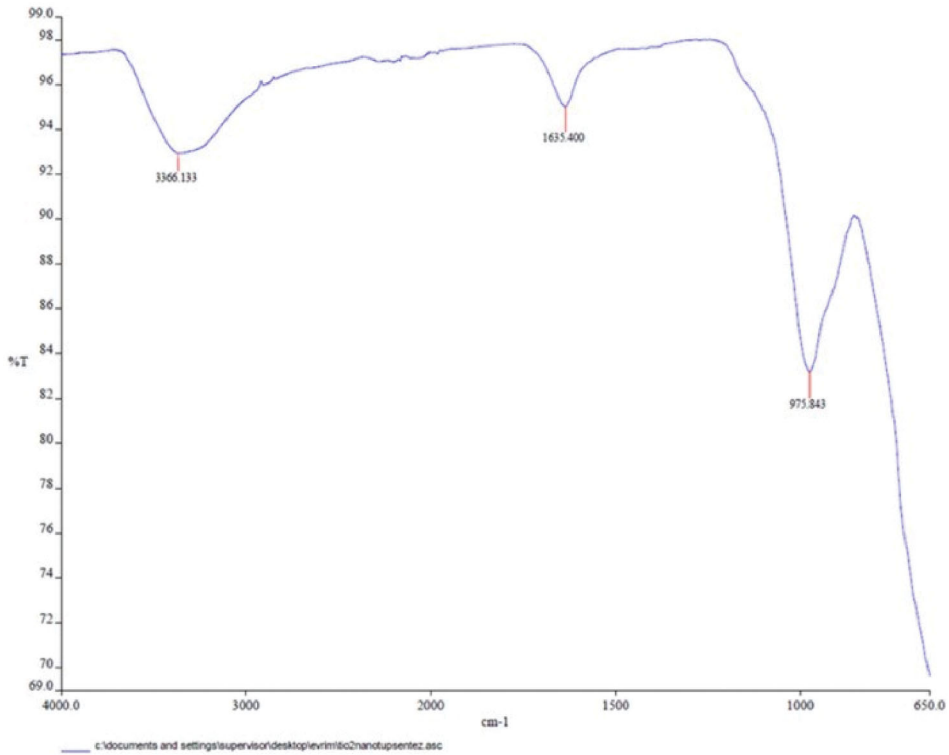


Figure 2. FTIR spectra of TiO<sub>2</sub>-n.

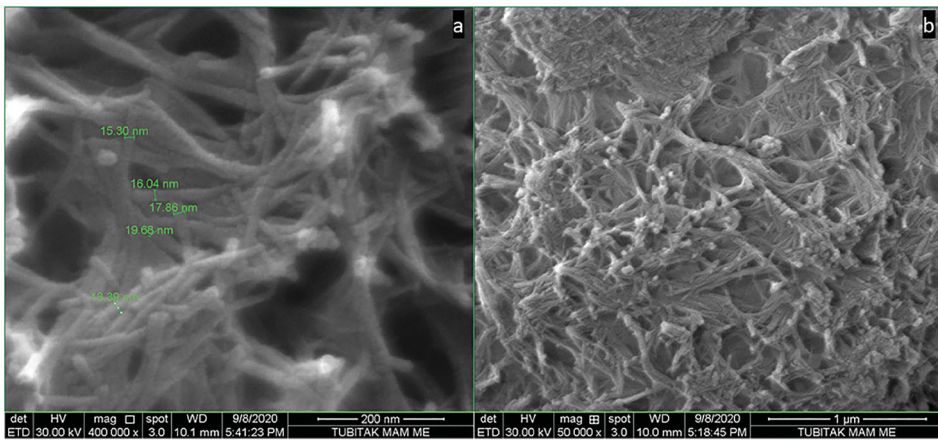


Figure 3. (a) SEM images of TiO<sub>2</sub>-n with × 400.000 magnification (b) SEM images of TiO<sub>2</sub>-n with × 50.000 magnification.

### 3.3. Surface roughness

The mean surface roughness and standard deviations obtained with a contact profilometer for all the tested composite resins are shown in Table 1. No significant difference was apparent between the surface roughness values of the control and TiO<sub>2</sub>-n groups ( $p > 0.05$ ).

**Table 1.** Mean surface roughness, standard deviation, and significant difference between the groups.

Surface roughness	Control Mean $\pm$ SD	0.1% TiO <sub>2</sub> -n Mean $\pm$ SD	0.5% TiO <sub>2</sub> -n Mean $\pm$ SD	1% TiO <sub>2</sub> -n Mean $\pm$ SD
	0.12 $\pm$ 0.03	0.20 $\pm$ 0.09	0.15 $\pm$ 0.03	0.25 $\pm$ 0.19
	A	A	A	A

Capital letters showed a significant difference between the groups.

**Table 2.** Mean microhardness values, standard deviation, and significant differences between the groups on the top and bottom surfaces.

Microhardness	Control Mean $\pm$ SD	0.1% TiO <sub>2</sub> -n Mean $\pm$ SD	0.5% TiO <sub>2</sub> -n Mean $\pm$ SD	1% TiO <sub>2</sub> -n Mean $\pm$ SD
Top	51.08 $\pm$ 1.71	56.4 $\pm$ 4.58	57.99 $\pm$ 4.34	59.41 $\pm$ 3.37
	Aa	ABa	Ba	Ba
Bottom	40.41 $\pm$ 1.37	38.35 $\pm$ 3.83	43.96 $\pm$ 2.24	37.59 $\pm$ 3.35
	ABb	ABb	Ab	Bb
<i>p</i>	0.004*	0.004*	0.004*	0.004*

Capital letters showed significant differences between the groups, lower letters showed significant differences between the bottom and top surfaces ( $p < 0.05$ ).

### 3.4. Microhardness results

Mean microhardness values, standard deviation, and significant differences between the groups on the top and bottom surfaces are provided in Table 2. The 1% TiO<sub>2</sub>-n and 0.5% TiO<sub>2</sub>-n groups showed significantly higher microhardness values compared to the control group on the top surfaces ( $p < 0.05$ ). No significant difference was determined among other groups ( $p > 0.05$ ). On the bottom surfaces, the highest microhardness value was obtained in the 0.5% TiO<sub>2</sub>-n group, and this value was significantly different from the 1% TiO<sub>2</sub>-n group ( $p < 0.05$ ). No significant difference was determined between other groups ( $p > 0.05$ ). In all groups, the top surfaces showed higher microhardness values than the bottom surfaces ( $p < 0.05$ ).

### 3.5. Three-point bending test

Mean three-point bending test results, standard deviations, and significant differences between the groups are presented in Table 3. The 0.5% TiO<sub>2</sub>-n group showed significantly higher three-point bending than the 1% TiO<sub>2</sub>-n group ( $p < 0.05$ ). No significant difference was observed between the other groups ( $p > 0.05$ ).

### 3.6. Analyses of fracture surfaces by SEM

Fracture surfaces of the 0.1% TiO<sub>2</sub>-n group are shown in Figure 4. A brittle-type fracture surface was observed, and spherical filler particles in the composite resin structure were seen. Nanotube structures were not seen directly as it was coated with polymer on the fracture surface and added at a low rate.

Fracture surfaces of the 0.5% TiO<sub>2</sub>-n group can be seen in Figure 5. At this level, the TiO<sub>2</sub>-n structures formed bridging to resist fracture against the force applied to the fracture surface during the three-point bending test (Figure 5(d)).

**Table 3.** Mean three-point bending, standard deviation, and significant difference between the groups.

	Control Mean ± SD	0.1% TiO <sub>2</sub> -n Mean ± SD	0.5% TiO <sub>2</sub> -n Mean ± SD	1% TiO <sub>2</sub> -n Mean ± SD
Three-point bending	106.98 ± 14.22 AB	119.15 ± 28.97 AB	116.82 ± 11.36 A	89.50 ± 14.22 B

Capital letters showed a significant difference between the groups.

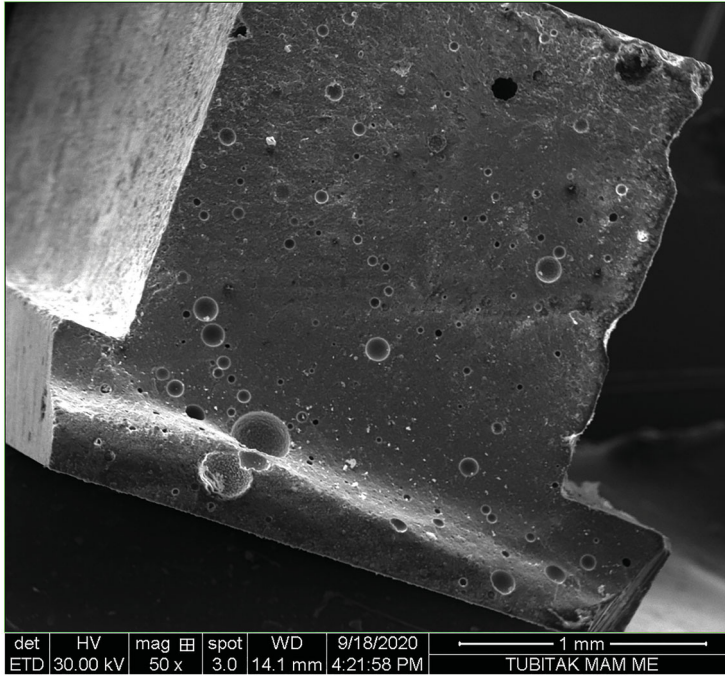


**Figure 4.** The fracture surface of 0.1% TiO<sub>2</sub>-n with × 50 magnification.

When the fracture surface belonging to the 1% TiO<sub>2</sub>-n group was examined, a brittle-ductile-type fracture surface was observed. A large number of porous structures in the area indicated by the arrow in Figure 6 indicates that polymerization is insufficient in the relevant regions of the composite surface. Spherical filler particles in the composite resin structure were also seen.

### 3.7. Antibacterial properties of the groups

The growth curves of the bacteria after the direct contact test are presented in Figures 7 and 8. No bacterial growth was observed in the negative control groups of any of the experimental groups. Positive control groups showed normal bacterial growth curves. The plateau stage refers to the stage at which bacterial growth becomes stable. There was no statistically significant difference in the mean plateau stage of *S.mutans* between the groups (18th hour;  $p > 0.05$ ; Figure 7).

There was a statistically significant difference between the groups in terms of average *L.casei* plateau stage (18th hour;  $p < 0.05$ ). It was observed that the 0.5% TiO<sub>2</sub>-n group had a statistically significantly lower value than the 0.1% TiO<sub>2</sub>-n, 1% TiO<sub>2</sub>-n,

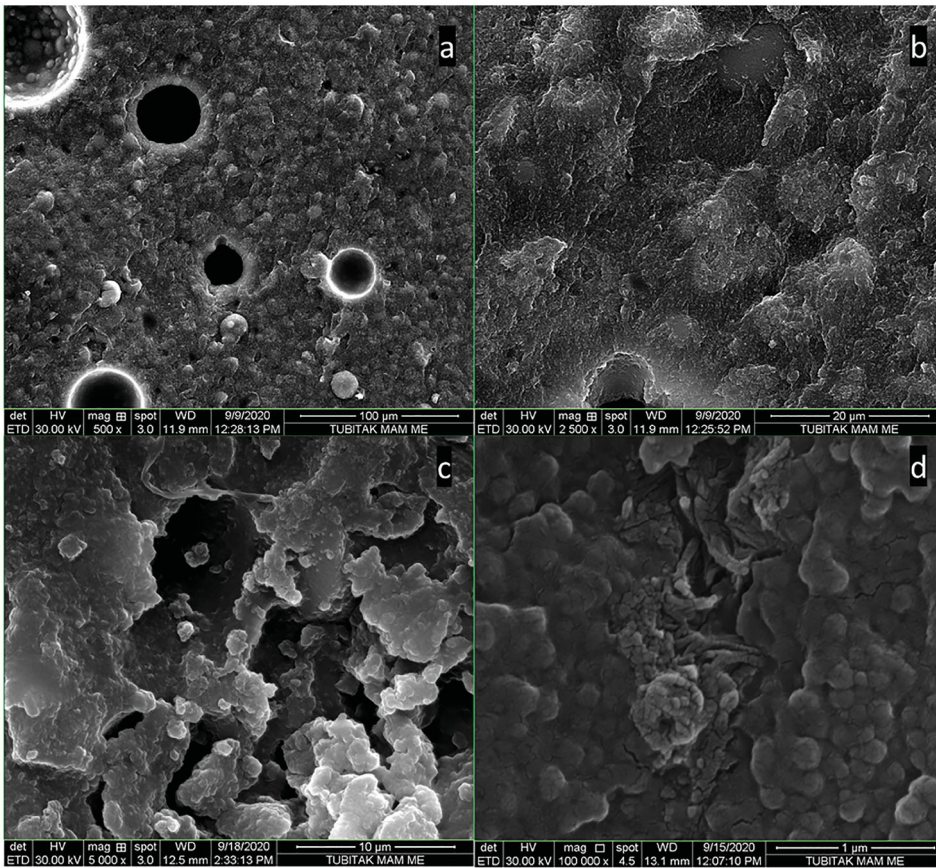


**Figure 5.** SEM image of the fracture surface belonging to the 0.5% TiO<sub>2</sub>-n (a)  $\times$  500 magnification (b)  $\times$  2.500 magnification (c)  $\times$  5.000 magnification (d)  $\times$  100.000.

and control groups. No significant difference was measured between the other groups ( $p > 0.05$ ).

#### 4. Discussion

To determine the mechanical properties of a low-viscosity bulk-fill composite with TiO<sub>2</sub>-n added at different rates, this study tested microhardness, surface roughness, and three-point bending. In addition, the antibacterial activity of bulk-fill composites with TiO<sub>2</sub>-n on *S.mutans* and *L.casei* was evaluated *via* the direct contact test. The results demonstrate that the addition of TiO<sub>2</sub>-n did not change the roughness of the low-viscosity bulk-fill composite; the addition of 0.5% and 1% TiO<sub>2</sub>-n increased the microhardness values of the composite; and the addition of 0.1% and 0.5% TiO<sub>2</sub>-n protected the three-point bending values, which increased slightly. When the direct contact test results were evaluated, the addition of TiO<sub>2</sub>-n did not show an antibacterial effect against *S.mutans*, but 0.5% TiO<sub>2</sub>-n resulted in an antibacterial effect against *L.casei* in daylight. Thus, the null hypothesis was partially accepted.

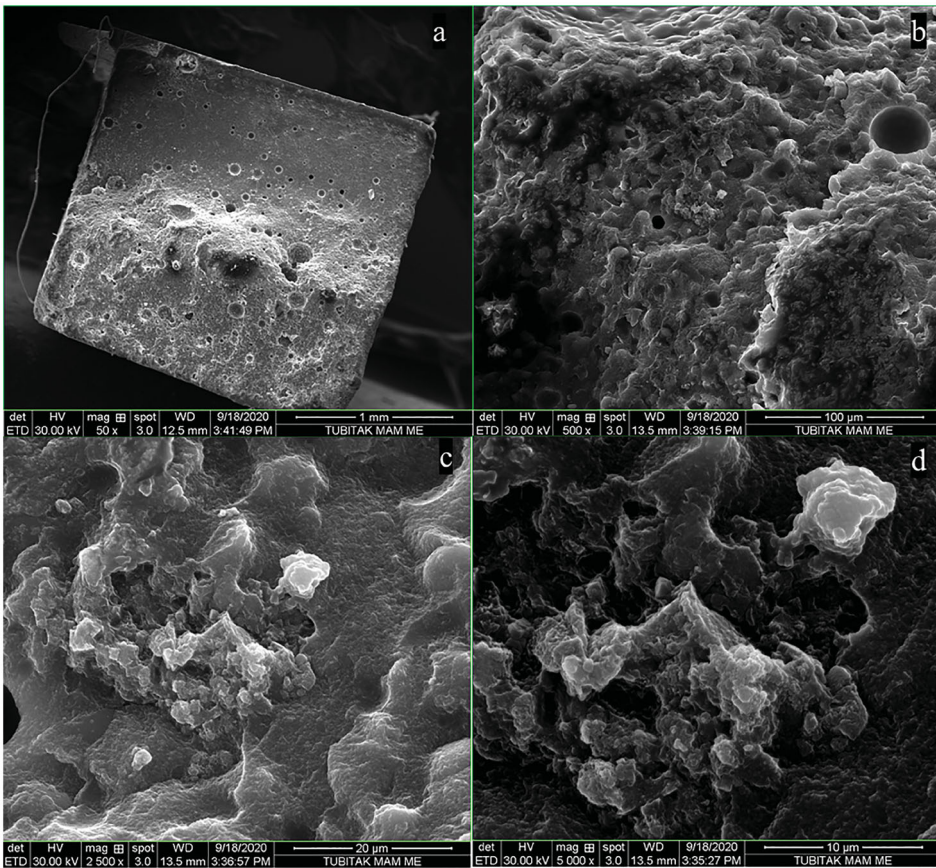


**Figure 6.** SEM image of the fracture surface belonging to the 1%  $\text{TiO}_2\text{-n}$  (a)  $\times 50$  magnification (b)  $\times 500$  magnification (c)  $\times 2,500$  magnification (d)  $\times 5,000$  magnification.

Titanium dioxide is one of the most studied metal oxides that is considered an anti-bacterial agent, and it improves the mechanical properties of materials. It is typically synthesized using the alkaline hydrothermal method. This method is advantageous because it produces pure phase nanostructures in a reproducible and cost-effective one-step reaction [36]. In the present study,  $\text{TiO}_2\text{-n}$  was synthesized by the hydrothermal method.

Lima et al. [37] noted that the polymerization of bulk-fill resin-based composites depends on material composition. Several studies have presented a reasonable depth of cure at 4 mm, confirming manufacturers' recommendations [38–40]. In contrast, other studies have related that several bulk-fill resin composites show sufficient polymerization but only until a depth of 2 or 3 mm [41,42]. In the present study, bulk-fill composites were prepared in Teflon molds with a 2 mm height. Although low-viscosity bulk-fill composites can be cured in a layer of 4 mm, it was thought that the filler ratio would increase with the addition of  $\text{TiO}_2\text{-n}$ , and thus the bottom surfaces would not sufficiently polymerize.

Patients can detect restorations with the tip of the tongue when the surface roughness is above  $0.3\ \mu\text{m Ra}$ . Studies have reported that the critical value of surface

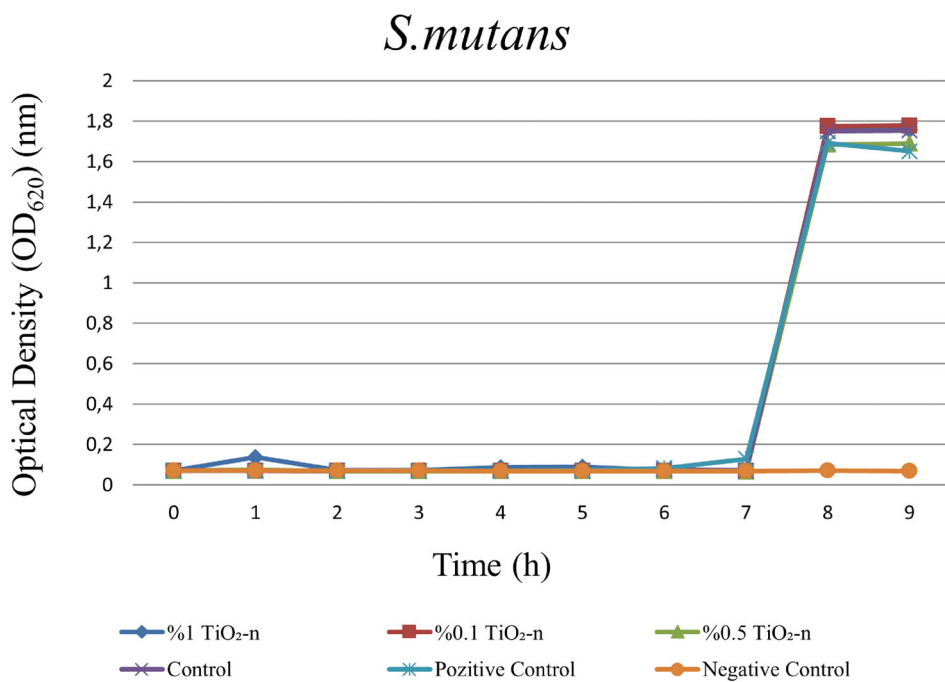


Figure 7. Growth curves for *S. mutans* after DCT with study and control groups.

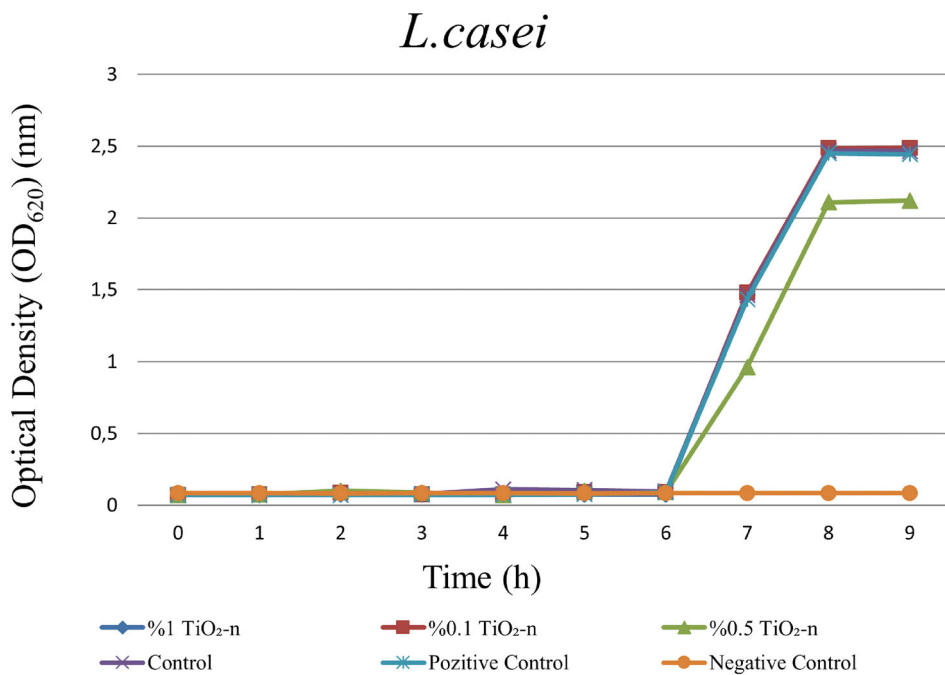


Figure 8. Growth curves for *L. casei* after DCT with study and control groups.

roughness in terms of bacterial involvement is  $0.20\ \mu\text{m}$  [43]. In the present study, it was observed that adding  $\text{TiO}_2\text{-n}$  in different proportions did not change the surface roughness of the bulk-fill composite. Although similar surface roughness values were found between the groups, the highest roughness value ( $0.25\ \mu\text{m}$ ) was obtained in the 1%  $\text{TiO}_2\text{-n}$  group, and this value exceeds the roughness limit in terms of bacterial involvement. The surface roughness of restorative materials depends on numerous factors, such as filler content, size, shape, monomer type, and an effective filler-organic matrix junction. In the present study, aluminum oxide polishing discs were used to finish and polish composite specimens. The abrasive particles of polishing systems must be harder than the fillers of composite resins for an effective finishing and polishing procedure. If they are not, the polishing system may remove only the soft resin matrix, leaving the filler particles protruding from the surface of the restorative material. In addition, insufficiently bonded fillers may debond and dislodge, leaving an irregular surface. It is possible that more drastically irregular surfaces observed with 1%  $\text{TiO}_2\text{-n}$  occurred due to poor bonding between  $\text{TiO}_2\text{-n}$  and the matrix and were left by the matrix after polishing.

Surface hardness, defined as the resistance to permanent indentation or penetration, is one of the most important properties used to compare restorative materials. This mechanical property of restorations should always be taken into account, especially when the restoration will face significant masticatory force. It has been reported that the shape, size, percentage by weight, composition, and distribution of filler particles in composite resins affect the hardness of the material [44]. Xia et al. coated the surface of  $\text{TiO}_2$  nanoparticles with organosilane and observed that 0.5% and 1%  $\text{TiO}_2$  nanoparticles increased the surface microhardness significantly. It is thought that an improvement in a material's microhardness is achieved by obtaining a more homogeneous surface as a result of surface modification. However, the agglomeration has also been observed despite surface modification [24]. Sun et al. [25] evaluated the effect of  $\text{TiO}_2$  nanoparticles modified with acrylic acid on the mechanical properties of an experimental composite resin. They observed the highest microhardness value at a rate of 0.06%  $\text{TiO}_2\text{-n}$ , and the mechanical properties of the composite were weakened at values above 1%  $\text{TiO}_2$  nanoparticles. Unlike previous studies, the present study performed the functionalization process of  $\text{TiO}_2\text{-n}$  using a different step instead of methacrylic acid during the production phase. Hydroxylic functional groups were obtained on the surface of the nanotubes during synthesis with a one-step reaction. The results of our study show that the addition of 0.5% and 1%  $\text{TiO}_2\text{-n}$  increased the microhardness of the top surface of low-viscosity bulk-fill composite, and the addition of  $\text{TiO}_2\text{-n}$  did not change the microhardness of the bottom surface. It has been reported that filler particles reflect polymerization light and prevent it from passing to the bottom surface [45]. In this study, similar microhardness values between the  $\text{TiO}_2\text{-n}$  groups and the control group on the bottom surfaces indicate that  $\text{TiO}_2\text{-n}$  did not affect the transmission of light to the bottom surfaces.

Heintze et al. [46] found that three-point bending and flexural modulus tests can be used as strong indicators of material durability under stress, and the results of these tests correlate well with clinical longevity. SEM observations reveal important information about the samples used and the mode of failure of the material. Lassila et al. [38]

reported that there is no direct relationship between filler volume and the three-point bending of composite resins, and they determined that the strength of adhesion between a filler particle and matrix may affect flexural strength. Panahandeh et al. [39] reported that higher three-point bending was found in composite resin with a lower percentage of filler. Xia et al. [24] evaluated the effect of TiO<sub>2</sub> nanoparticles on the three-point bending of composites, and similar three-point bending results were observed between the 0.5% TiO<sub>2</sub> nanoparticle group and the control group. However, a significant increase was observed in the group containing 1% TiO<sub>2</sub> nanoparticles [24].

Sun et al. [25] evaluated the effect of adding 0.02%–0.5% TiO<sub>2</sub> nanoparticles modified with acrylic acid to the experimental composite resin, finding that the lowest three-point bending value was 0.5% and the highest 0.06%. Sun et al. suggested that the decrease in three-point bending despite the increase in concentration may have occurred due to the agglomeration of TiO<sub>2</sub> nanoparticles and insufficient polymerization at this concentration level. In contrast with previous studies, the present study observed similar three-point bending values between groups. Adding TiO<sub>2</sub>-n did not change the three-point bending of the bulk-fill composite. The unique results observed in our study compared to previous studies may be due to the different modifications applied to the surfaces of TiO<sub>2</sub>-n.

According to the International Organization for Standardization (ISO 4049: 2009) [34], the three-point bending of composite resin to be used in the posterior occlusal region should not be less than 80 MPa [47]. The three-point bending values obtained in this study varied between 88–118 MPa, thereby consistently exceeding 80 MPa. The highest three-point bending value belonged to the group containing 0.5% TiO<sub>2</sub>-n (118.76 MPa), while the lowest value was observed in the 1% TiO<sub>2</sub>-n group (88.07 MPa). Although there was no statistical difference, the decrease observed in the 1% TiO<sub>2</sub>-n group may have resulted from the increased tendency for agglomeration with the increase in TiO<sub>2</sub>-n ratio; this change may adversely affect material durability by causing voids and irregularities. The three-point bending test results were supported by the SEM examination. Non-polymerized irregular areas were observed in the 1% group in the examination of fracture surfaces. In the 0.5% TiO<sub>2</sub>-n group, it was observed that the nanotube structures bridged at the fracture surface to resist breaking against the force applied during the flexural strength test. The bridging structures observed on the fracture surfaces indicate a strong connection between TiO<sub>2</sub>-n and the matrix.

While many studies have investigated the effect of antibacterial activity of TiO<sub>2</sub>-n against *S.mutans*, only a limited number of studies have assessed its effect against *L.casei*. In the present study, the antibacterial activity of composites with TiO<sub>2</sub>-n was evaluated against *S.mutans* and *L.casei*, which play an important role in the formation and progression of caries. Dias et al. [40] synthesized nanoparticles using the polymeric precursor and hydrothermal method and then added the nanoparticles to the composite resin at different rates. Antibacterial activity was not observed against *S.mutans* with the nanoparticles produced by the hydrothermal method, but nanoparticles produced by polymeric precursor did demonstrate antibacterial activity against *S.mutans*. In the present study, TiO<sub>2</sub>-n was synthesized *via* the hydrothermal method, and the low-viscosity bulk-fill composite with TiO<sub>2</sub>-n did not show antibacterial activity against

*S.mutans* as a result. However, antibacterial activity was observed against *L.casei* in the group containing 0.5% TiO<sub>2</sub>-n. We believe that the antibacterial activity observed in the present study with low TiO<sub>2</sub>-n concentration in daylight is related to the morphology of TiO<sub>2</sub>-n, which resulted from the synthesis method used.

Cai et al. [41] evaluated the antibacterial activity of composite resin with TiO<sub>2</sub> nanoparticles under UV light treatment, and the UV-applied group exhibited more effective antibacterial behavior than the non-UV group. Jing et al. [48] investigated the antibacterial activity of TiO<sub>2</sub> nanoparticles and nanotubes produced by the sol-gel method against *E.coli*. They reported that TiO<sub>2</sub> nanoparticles exhibited higher antibacterial activities than TiO<sub>2</sub>-n under UV light treatment, but the two offered similar antibacterial activities in the dark due to changes in their microstructure. Jing et al. also noted that both TiO<sub>2</sub> nanoparticles and TiO<sub>2</sub>-n have less antibacterial activity in the dark than under UV light. Currently, the UV energy doses required for adequate antibacterial efficacy are highly dangerous to human cells and tissues, so there are concerns regarding the use of this technology in the oral cavity [49]. Because of these negative features, we used laboratory light instead of UV light when conducting the direct contact test in this study.

There are certain limitations to our study. The mechanical properties of bulk-fill composites were evaluated by performing static tests such as three-point bending, microhardness, and roughness. Radiopacity, optical properties, color change, water absorption, water solubility, viscosity assessment, wettability, and conversion degree of composite resins were not evaluated. Instead of the sol-gel method, the hydrothermal synthesis method was utilized due to its ease of application and other advantages. The functionalization process of TiO<sub>2</sub>-n was carried out using a different step instead of methacrylic acid during the production phase. Future studies are needed that photocatalyst TiO<sub>2</sub>-n under visible light without UV application. The release of TiO<sub>2</sub>-n into oral tissues and saliva and its effect on bacterial adhesion was not evaluated in this study but should be addressed in future studies.

## 5. Conclusion

This *in vitro* study evaluated the effect of the addition of different proportions of TiO<sub>2</sub>-n to a low-viscosity bulk-fill composite resin on the mechanical and antibacterial properties of the composite.

1. The addition of TiO<sub>2</sub>-n did not alter the surface roughness of the low-viscosity bulk-fill composite resin.
2. Adding 0.5% and 1% TiO<sub>2</sub>-n increased the microhardness of the low-viscosity bulk-fill composite resin on the top surface.
3. The addition of 0.1% and 0.5% TiO<sub>2</sub>-n protected the three-point bending values, which showed a slight increase, of the low-viscosity bulk-fill composite.
4. Although antibacterial activity was not observed for *S.mutans*, inclusion of 0.5% TiO<sub>2</sub>-n in the low-viscosity bulk-fill composite resin did produce an antibacterial effect against *L.casei* in daylight.

## Acknowledgments

Many thanks to Yıldız Technical University Advanced Materials Research Group (YTU-AMRG) for all contributions that are made in the course of the study. Many thanks to Assistant Professor Sevilay Karahan for her help with statistical analyses. A part of this study has been presented in 10th Cons Euro 2021 and was published in *Clinical Oral Investigations* vol 25, pages 4185-4238 (2021). Hence, this study should be considered as a continuation of the authors previous conference proceedings.

## Disclosure statement

The authors have no patented, monetary, or other personal interest of any nature or type in any product, service, and/or company that is presented in this article.

## Funding


This study was funded by Bezmialem Vakıf University Scientific Research Projects Unit (11.2018/13, 12.2018/10). The funders had no role in the design, conduction, evaluation or interpretation of the study, or in writing the manuscript. The authors do not have any financial interest in the companies whose materials are included in this article.

## ORCID

Evrin Eliguzelolu Dalkilic  <http://orcid.org/0000-0002-1075-9278>

Bedri Onur Kucukyildirim  <http://orcid.org/0000-0002-0399-5467>

Ayşegül Akdoğan Eker  <http://orcid.org/0000-0003-0212-9230>

Nursen Topcuoğlu  <http://orcid.org/0000-0002-5041-1129>

Güven Kulekci  <http://orcid.org/0000-0002-7391-1310>

## References

- [1] Alshali RZ, Salim NA, Satterthwaite JD, et al. Long-term sorption and solubility of bulk-fill and conventional resin-composites in water and artificial saliva. *J Dent.* 2015; 43:1511–1518.
- [2] El-Safty S, Silikas N, Watts DJ. Creep deformation of restorative resin-composites intended for bulk-fill placement. *Dent Mater.* 2012;28:928–935.
- [3] Shah PK, Stansbury JW. Photopolymerization shrinkage-stress reduction in polymer-based dental restoratives by surface modification of fillers. *Dent Mater.* 2021;37: 578–587.
- [4] Ilie N, Hickel RJ. Silorane-based dental composite: behavior and abilities. *Dent Mater J.* 2006;25:445–454.
- [5] Abbas G, Fleming G, Harrington E, et al. Cuspal movement and microleakage in pre-molar teeth restored with a packable composite cured in bulk or in increments. *J Dent.* 2003;31:437–444.
- [6] Czasch P, Ilie N. In vitro comparison of mechanical properties and degree of cure of bulk-fill composites. *Clin Oral Investig.* 2013;17:227–235.
- [7] Ilie N, Bucuta S, Draenert M. Bulk-fill resin-based composites: an in vitro assessment of their mechanical performance. *Op Dent.* 2013;38:618–625.
- [8] Jin X, Bertrand S, Hammesfahr PD. New radically polymerizable resins with remarkably low curing stress. *J Dent Res.* 2009;88:1651.

- [9] Kim RJY, Kim YJ, Choi NS, et al. Polymerization shrinkage, modulus, and shrinkage stress related to tooth-restoration interfacial debonding in bulk-fill composites. *J Dent.* 2015;43:430–439.
- [10] Sakaguchi RL. Review of the current status and challenges for dental posterior restorative composites: clinical, chemistry, and physical behavior considerations. *Dent Mater.* 2005;21:3–6.
- [11] Mjör IA, Moorhead JE, Dahl JE. Reasons for replacement of restorations in permanent teeth in general dental practice. *Int Dent J.* 2000;50(6):361–366.
- [12] Bernardo M, Luis H, Martin MD, et al. Survival and reasons for failure of amalgam versus composite posterior restorations placed in a randomized clinical trial. *J Am Dent Assoc.* 2007;138(6):775–783.
- [13] Drummond JL. Degradation, fatigue, and failure of resin dental composite materials. *J Dent Res.* 2008;87(8):710–719.
- [14] Demarco FF, Collares K, Correa MB, et al. Should my composite restorations last forever? Why are they failing? *Braz Oral Res.* 2017;31(suppl 1):e56.
- [15] Padovani GC, Fucio S, Ambrosano GM, et al. *In situ* bacterial accumulation on dental restorative materials. CLSM/COMSTAT Analysis. *American J Dent.* 2015;28:3–8.
- [16] Konishi N, Torii Y, Kurosaki A, et al. Confocal laser scanning microscopic analysis of early plaque formed on resin composite and human enamel. *J Oral Rehabil.* 2003;30(8):790–795.
- [17] Nedeljkovic I, Teughels W, De Munck J, et al. Is secondary caries with composites a material-based problem? *Dent Mater.* 2015;31:e247–277.
- [18] Kawashita M, Tsuneyama S, Miyaji F, et al. Antibacterial silver-containing silica glass prepared by sol-gel method. *Biomaterials.* 2000;21:393–398.
- [19] Salman TA, Khalaf HA. The influence of adding of modified ZrO<sub>2</sub>-TiO<sub>2</sub> nanoparticles on certain physical and mechanical properties of heat polymerized acrylic resin. *J Baghdad Collage Dent.* 2015;27:33–39.
- [20] Tolou NB, Fathi M, Monshi A, et al. The effect of adding TiO<sub>2</sub> nanoparticles on dental amalgam properties. *Iran J Mater Sci& Engi.* 2013;10:46–56.
- [21] Ai M, Du Z, Zhu S, et al. Composite resin reinforced with silver nanoparticles-laden hydroxyapatite nanowires for dental application. *Dent Mater.* 2017;33:12–22.
- [22] Goto K, Tamura J, Shinzato S, et al. Bioactive bone cements containing nano-sized titania particles for use as bone substitutes. *Biomaterials.* 2005;26:6496–6505.
- [23] Moszner N, Salz UJ. New developments of polymeric dental composites. *Progress Polym Sci.* 2001;26:535–576.
- [24] Xia Y, Zhang F, Xie H, et al. Nanoparticle-reinforced resin-based dental composites. *J Dent.* 2008;36:450–455.
- [25] Sun J, Forster AM, Johnson PM, et al. Improving performance of dental resins by adding titanium dioxide nanoparticles. *Dent Mater.* 2011;27:972–982.
- [26] Dafar MO, Grol MW, Canham PB, et al. Reinforcement of flowable dental composites with titanium dioxide nanotubes. *Dent Mater.* 2016;32(6):817–826.
- [27] Poosti M, Ramazanzadeh B, Zebarjad M, et al. Shear bond strength and antibacterial effects of orthodontic composite containing TiO<sub>2</sub> nanoparticles. *Eur J Orthod.* 2013;35:676–679.
- [28] Elsaka SE, Hamouda IM, Swain MV. Titanium dioxide nanoparticles addition to a conventional glass-ionomer restorative: influence on physical and antibacterial properties. *J Dent.* 2011;39:589–598.
- [29] Acosta-Torres LS, López-Marín LM, Nunez-Anita RE, et al. Biocompatible metal-oxide nanoparticles: nanotechnology improvement of conventional prosthetic acrylic resins. *J Nanomaterials.* 2011;8:2011.
- [30] Pinto D, Bernardo L, Amaro A, et al. Mechanical properties of epoxy nanocomposites using titanium dioxide as reinforcement—a review. *Construc and Build Mater.* 2015;95:506–524.

- [31] Cheng L, Zhang K, Weir MD, et al. Nanotechnology strategies for antibacterial and remineralizing composites and adhesives to tackle dental caries. *Nanomedicine (Lond)*. 2015;10:627–641.
- [32] Li Q, Mahendra S, Lyon DY, et al. Antimicrobial nanomaterials for water disinfection and microbial control: potential applications and implications. *Water Res*. 2008;42:4591–4602.
- [33] Sun J, Watson SS, Allsopp DA, et al. Tuning photo-catalytic activities of TiO<sub>2</sub> nanoparticles using dimethacrylate resins. *Dent Mater*. 2016;32:363–372.
- [34] ISO 4049. Dentistry-Polymer-Based restorative materials. International Organization for Standardization. 2009;4:1–28.
- [35] Lassila L, Keulemans F, Vallittu PK, et al. Characterization of restorative short-fiber reinforced dental composites. *Dent Mater J*. 2020;39:992–999.
- [36] Ou HH, Lo SL. Review of titania nanotubes synthesized via the hydrothermal treatment: fabrication, modification, and application. *Separ Purific Tech*. 2007;58:179–191.
- [37] Lima RB, Troconis CC, Moreno MB, et al. Depth of cure of bulk fill resin composites: a systematic review. *J Esth Rest Dent*. 2018;30:492–501.
- [38] Zorzin J, Maier E, Harre S, et al. Bulk-fill resin composites: polymerization properties and extended light curing. *Dent Mater*. 2015;31:293–301.
- [39] Kelić K, Matić S, Marović D, et al. Microhardness of bulk-fill composite materials. *Acta Clin Croat*. 2016;55:607–614.
- [40] Lapas-Barisic M, Gamulin O, Panduric V, et al. Long term degree of conversion of two bulk-fill composites. *Acta Stomatol Croat*. 2016;50:292–300.
- [41] Yap AU, Pandya M, Toh WS. Depth of cure of contemporary bulk-fill resin-based composites. *Dent Mater J*. 2016;35:503–510.
- [42] Garcia D, Yaman P, Dennison J, et al. Polymerization shrinkage and depth of cure of bulk fill flowable composite resins. *Oper Dent*. 2014;39:441–449.
- [43] Antonson SA, Yazici AR, Kilinc E, et al. Comparison of different finishing/polishing systems on surface roughness and gloss of resin composites. *J Dent*. 2011;39:e9–e17.
- [44] Kim KH, Ong JL, Okuno OJ. The effect of filler loading and morphology on the mechanical properties of contemporary composites. *J Prosth Dent*. 2002;87:642–649.
- [45] Khaled S, Miron RJ, Hamilton DW, et al. Reinforcement of resin based cement with titania nanotubes. *Dent Mater*. 2010;26(2):169–178.
- [46] Heintze S, Forjanic M, Rousson VJ. Surface roughness and gloss of dental materials as a function of force and polishing time *in vitro*. *Dent Mater*. 2006;22(2):146–165.
- [47] Huang Q, Huang S, Liang X, et al. The antibacterial, cytotoxic, and flexural properties of a composite resin containing a quaternary ammonium monomer. *J Prosth Dent*. 2018;120:609–616.
- [48] Jing Z, Guo D, Wang W, et al. Comparative study of titania nanoparticles and nanotubes as antibacterial agents. *Solid State Sci*. 2011;13:1797–1803.
- [49] Florez FL, Hiers RD, Larson P, et al. Antibacterial dental adhesive resins containing nitrogen-doped titanium dioxide nanoparticles. *Mater Sci Eng C Mater Biol Appl*. 2018;93:931–943.